ORIGINAL PAPER

CHARACTERIZATION OF AIRBORNE PARTICULATE MATTER TO ASSESS THE IMPACT ON DEGRADATION OF CULTURAL HERITAGE: THE TROPAEUM TRAIANI MONUMENT

CRISTIANA RADULESCU[1,2], RODICA MARIANA ION[3,4], CLAUDIA STIHI[1,2], IOANA DANIELA DULAMA[1*], CRISTINA MIHAELA NICOLESCU[1], IOAN ALIN BUCURICA[1], ION VALENTIN GURGU[1], RALUCA MARIA STIRBESCU[1], RADU LUCIAN OLTEANU[1], SORINA GEANINA STANESCU[1], ANCA IRINA GHEBOIANU[1], DORIN DACIAN LET[1], SOFIA TEODORESCU[1], LIVIU OLTEANU[1], NICOLAE MIHAIL STIRBESCU[1]

Manuscript received: 15.07.2021; Accepted paper: 12.08.2021;
Published online: 30.09.2021.

Abstract. *The present paper is focused on the microclimatic investigation and weather-climatic phenomena matrix assessment, which can be generated for heritage objectives at different spatial and temporal resolutions, correlated with physicochemical analysis of the particulate matter ($PM_{2.5-10}$). In the literature the importance of atmospheric PM monitoring in the proximity of monuments is not yet sufficiently highlighted. In this respect, the microclimatic investigation of the Tropaeum Traiani Monument (Adamclisi, Romania) was performed to assess the suitability of a closed environment, located outdoors, according to the conservation requirements of heritage materials. The monitoring campaigns (four seasons, e.g., from summer of the year 2018 to spring of the year 2019) were carried out by non-invasive measuring equipment. The collected data were used to investigate the hygrothermal and chemical behavior inside and outside of Tropaeum Traiani Monument, built in 109, to assess the risks on the oldest structural material. Principal component analysis (PCA) was performed by IBM SPSS Statistics software to assess the similarities between the microclimatic parameters.*

Keywords: *Tropaeum Traiani Monument; weather-climatic phenomena; particulate matter; ICP-MS; ATR-FTIR.*

INTRODUCTION

Tropaeum Traiani is a monument in *Roman Civitas Tropaensium* (site of modern Adamclisi, Romania), built in 109 in then Moesia Inferior, to commemorate Roman Emperor Trajan's victory over the Dacians, in the winter of 101–102, in the Battle of Adamclisi [1]. Outside, on the monument walls were 54 metopes depicting Roman legions fighting against enemies [2-4]; most of these metopes are preserved in the nearby museum. Thus, there are six

[1] Valahia University of Targoviste, Institute of Multidisciplinary Research for Science and Technology, 130004 Targoviste, Romania. *Corresponding Author:* dulama_id@yahoo.com
[2] Valahia University of Targoviste, Faculty of Sciences and Arts, 130004 Targoviste, Romania. E-mail: radulescucristiana@yahoo.com
[3] Valahia University of Targoviste, Faculty of Materials Engineering and Mechanics, 130004 Targoviste, Romania.
[4] National Institute of Research and Development for Chemistry and Petrochemistry – ICECHIM, 060021 Bucharest, Romania.

segments describing chronologically the events of the Dacian Wars [5] and similar themes are found in the plastic compositions of the Trajan's Column (I - the Roman cavalry assault, the fight with infantry; II - the preparation of the Roman infantry attack; III - the Roman infantry fight at plain with Dacian pedestrians; IV - the speech to victorious infantry; V - the fight of the infantry on the heights and in the forest; and VI - submission of the defeated population, leadership of the war prisoners in front of the Emperor) [5]. In the 20th century, the monument was reduced to a mound of stone and mortar, with a large number of the original bas-reliefs scattered around [2]. The present edifice is a reconstruction, dating from 1977, after one of the hypothetical models of the old monument ruins.

It is obvious that any rehabilitation of a historical monument must be carried out following a careful study of the location where the monument is found, the weather conditions and global climate changes [6], the pollution degree [7,8], extreme risk cases (earthquakes [9], sea storms, arid or salty marine conditions [10], microbes [11] and dangerous vegetation [12], such as molds, perennial plants etc.). Furthermore, monument rehabilitation is a special issue that involves the study of effects that cause surface damage of monument structures, in order to search the relevant restoration materials and methods to preserve them against climatic changes and pollution, as well [13,14].

The chemical composition of particulate matter (PM) is well known [15-20] and mainly contains: trace elements (heavy and radioactive metals, such as Ag, As, Ba, Be, Dc, Ce, Cr, Co, Cu, Fe, Mn, Nd, Ni, Pb, Sb, Se, Sr, Ti, V and Zn) in oxides or inorganic salts (e.g. sulfate, sulfide, nitrate, carbonate, silicate, chloride), water, organic substances, black carbon, mineral dust and other components of the earth's crust, as well as low concentrations of various species, including bioactive organic compounds and redox cycling metals. Both short-term timeseries and long-term studies [15, 21, 22] have included the sulfate and sulfite content from particulate matter as a specific variable in effect analysis on health and environment. There are some possible direct processes through which sulfate and nitrate anions from $PM_{2.5\text{-}10}$, corroborated with high temperature [23, 24], may affect heritage-related endpoints [25], including interactions with some metals [26], that may lead to the production of secondary organic compounds [27, 28]. Further free radicals such as $SO_2\cdot$ and irritant peroxyacetyl nitrates (PAN) are dangerous to structural material of old historical monuments [29]. The deposition of PM inside of rehabilitated old monuments strongly depends on particle size and is governed by the processes of particle diffusion toward the old structures, which is of particular significance for small particles (PM with size less than 10 µm), and of gravitational sedimentation, which is significant for larger particles (PM with size high than 10 µm).

The research work represents the first comprehensive microclimate assessment in the Tropaeum Traiani Monument ever carried out, with the scope to analyze in detail the possible risks for the original monument itself. The first stage of this research was to identify climatic and microclimatic risk factors during to the year of 2018, the causes (*i.e.*, pollution) and the potential consequences (*e.g.*, chemical, physical and microbiological degradation) on the original archaeological substrates of Tropaeum Traiani Monument. Environmental conditions (inside and outside) can significantly influence the degradation processes of the materials, and the effects of these processes was observed and classified on different levels, as well. The elemental composition of PM samples was determined by inductively coupled plasma mass spectrometry. Fourier transform infrared spectroscopy is an analytical technique that captures the signature of a multitude of PM constituents that give rise to feature-rich spectral patterns over the mid-infrared (mid-IR) wavelengths [30-33]. The qualitative information regarding the abundance of inorganic ions and organic compounds in PM was an important issue in the choosing of FTIR as tool for the first diagnose of degradation stage of the original materials of the monument.

2. MATERIALS AND METHODS

The research shows the results of an in-field experimental campaign carried out through non-invasive measuring instruments, such as: PCE FWS20 weather station, Voltcraft SL-100 sonometer, Solar Light PMA2100 and TE-Wilbur low-volume air particulate matter sampler, equipped with polytetrafluoroethylene (PTFE) filters (d = 0.45 μm, Φ = 47 mm) for particle sampling. These filters were chosen due the fact that relatively cleanest IR absorbance spectrum will be obtained [15]. The monitoring campaign was performed during of the summer of the year 2018 to spring of the year 2019. For each season were chosen the last month of season (August for summer, November for autumn, February for winter and May for spring). The campaign was carried out 24 hours/7 days/season/risk period (a very warm month and the rainy, cold month), also taking in account the meteorological predictions.

The analysis and quantification of trace elements (*i.e.*, Cu, Pb, Zn, Cr, Cd, Al, Ni, Fe and Mn) in PM samples (*i.e.*, 7 samples/season) was performed by inductively coupled plasma - mass spectroscopy (ICP-MS) using iCAP™ Qc device [15,17]. For ICP-MS analysis, the samples were digested in HNO_3 on a hot plate by using a TOPwave Microwave-assisted pressure system [16,19]. All chemical reagents were of analytical grade. For ICP-MS technique the quantification was performed by standard curve; metals calibration curves showed good linearity over the concentration range (0.1 to 10.0 $mg \cdot L^{-1}$), with R^2 correlation coefficients in the range of 0.996 to 0.999. The measurements were performed in triplicate. Standard reference material (*i.e.*, NIST SRM 1648a, Urban Particulate Matter) was used to verify the accuracy and traceability of the method. The relative standard deviation (RSD) of standard was 0.36%, the RSD of samples was 1.2%–2.4%, and the recovery rate was 93.5%-103.2%.

Molecular identification of chemical functional groups of inorganic and organic compounds deposited on filters was performed by attenuated total reflection – Fourier transform infrared spectroscopy (ATR-FTIR) using Vertex 80v spectrometer (Bruker), equipped with diamond ATR crystal accessory, for high refractive index bulk sample, as well as with HYPERION microscope. The ATR-FTIR spectroscopy has limited applications in quantitative research, since it has a penetration depth of only a few microns, but for qualitative investigation could be a suitable technique. The ATR-FTIR method did not require special preparation of samples. The blank was handled exactly as each sample filter from pre-scan until the final analysis was completed. Samples were chosen based on their black color and thickness (~2 mm), being placed into 47 mm Petri Dishes. The “thick” spectra (recorded from seven samples/season of PM collected on filter) were analyzed in the range of 4000–400 cm^{-1} (being representative for what can generally be obtained from $PM_{2.5–10}$ particles) by nondestructive transmission FTIR spectroscopy.

Descriptive, associative, and comparative statistics of the recorded time series were analyzed using IBM SPSS Statistics (software version 21) for MS Windows. The computation of multiple range tests provided the statistical significance of comparisons between season parameters (*e.g.*, temperature, humidity, absolute pressure, wind speed and dew point) and locations (*i.e.*, inside, and outside of the monument). Principal component analysis (PCA) by Component plot in rotated space of microclimate parameters was performed, according with on Varimax with Kaiser normalization to reduce the number of factors that explains the variability in air pollution from historical studied area. The input matrix began with two seasons (i.e., summer and autumn) by five variables (*i.e.*, temperature, humidity, absolute pressure, wind speed and dew point).

3. RESULTS AND DISCUSSION

Air temperature and relative humidity are key variables of research in the field of environmental protection. Both parameters are hard to monitor, especially on a national scale, due to spatial heterogeneity. The temperature is expected to increase in this century, considering the climatic changes and knowing that in 2017, the recorded value was 53.7°C. The minimum and maximum variations of temperature influenced the degradation process of the original materials. It is well-known that organic and inorganic materials are extremely sensitive to thermo-hygrometric cycles, especially to the shorter ones (*i.e.*, daily cycles, repeatedly dilated/contracted). They generate steep gradients starting from the outer surface of the object, giving rise to inner tensions which result in dimensional variations and may lead to irreversible changes in chemical composition of the original materials. Excessive humidity observed inside the monument (100% in two days of monitoring campaign of the end of August 2018), accelerated the harmful effect of atmospheric pollutants and other toxic substances which irreversibly accentuating the degradation process. At the opposite end, during the cold season when humidity was lower inside the monument, efflorescence (*e.g.*, *Xantoria parietina*, *Dicarnum scoparium*, *Cynodon dactylon*, *Poa annua*, *Bellis perennis*, and *Taxacum oficinale*) was observed on the original materials, explained by high salt content (60 km from Black Sea). In addition, with temperature and humidity (inside and outside), wind speed, dew point, and atmospheric pressure (outside) were monitored. In conclusion, even if an outside confined environment may not be suitable for conservation of the original heritage materials, depending on the climatic region, several solutions can be proposed to reduce the impact of the external climatic risk. Consequently, the thermo-hygrometric variation inside the monument shortens the durability of the preserved materials.

Table 1 and Fig. 1 present a descriptive statistic of microclimate parameters measured one week per season, inside and outside.

Based on these parameters, to evaluate the correlation between microclimate parameters measured outside in both summer and autumn seasons, the IBM SPSS Statistics software – Principal Component Analysis (PCA) was used. The component plot in rotated space (Fig. 2) shows a good correlation between temperature and dew point (*i.e.*, Ta–Da and Ts–Ds) on both monitored seasons, absolute pressures (*i.e.*, Pa–Ps) and wind speed (i.e. Wa–Ws). The correlation matrix of microclimate parameters measured outside in both summer and autumn seasons (Table 2) highlights a strong correlation between temperature, dew point and humidity (i.e., Ts–Hs, Ts–Ds, Ta–Da and Hs–Ds) and also, between absolute pressures (*i.e.*, Pa–Ps). A good correlation (> 0.7) was observed between temperature, absolute pressure, dew point and wind speed (*i.e.*, Ts–Ps, Ta–Wa, Ps–Ds, Wa–Da and Hs–Ws).

Air quality in the locations of the studied heritage site is influenced by several categories of sources of pollution, such as: local and/or transient (*i.e.*, tourist visits) road traffic; agricultural / industrial activities carried out around adjacent areas; domestic activities. Linked to pollution sources, the main pollutants are nitrogen oxides, carbon oxides, sulfur oxides, volatile and condensable organic compounds, heavy metals, and suspended particulate matter ($PM_{2.5–10}$). Inside of the historical monument, the organic compounds and soot in PM, deteriorated the surface of old ruins, behave a very attractive medium for SO_2 capture (this was observed by soiling the structure surface) [23].

Table 1. Descriptive statistics of microclimate parameters measured one week per season, inside and outside.

	Parameter	Min.	Max.	Mean	Median	S.D.
Summer	*INSIDE*					
	Temperature [°C]	22.80	34.40	27.77	28.10	2.93
	Humidity [%]	75.00	94.00	82.78	81.00	5.16
	OUTSIDE					
	Temperature [°C]	16.20	35.10	25.12	25.40	4.81
	Humidity [%]	24.00	95.00	55.22	56.00	16.52
	Absolute pressure [mmHg]	745.70	752.90	748.61	748.30	2.19
	Wind speed [m/s]	0.00	7.50	1.56	1.00	1.43
	Dew point [°C]	9.40	20.70	14.64	14.20	2.16
Autumn	*INSIDE*					
	Temperature [°C]	2.00	5.40	3.91	4.10	0.85
	Humidity [%]	84.00	99.00	91.51	92.00	3.03
	OUTSIDE					
	Temperature [°C]	-2.50	5.40	1.33	1.80	1.86
	Humidity [%]	76.00	99.00	94.09	95.00	5.35
	Absolute pressure [mmHg]	744.30	754.30	749.81	749.60	2.68
	Wind speed [m/s]	0.00	8.20	2.23	1.70	1.76
	Dew point [°C]	-3.40	5.30	0.50	0.55	2.08
Winter	*INSIDE*					
	Temperature [°C]	3.60	12.10	7.99	7.60	2.34
	Humidity [%]	80.00	97.00	88.21	88.00	3.82
	OUTSIDE					
	Temperature [°C]	-0.20	17.40	7.20	5.85	4.46
	Humidity [%]	31.00	99.00	70.24	73.00	17.81
	Absolute pressure [mmHg]	744.50	751.70	748.66	749.35	2.31
	Wind speed [m/s]	0.00	6.10	2.08	1.70	1.35
	Dew point [°C]	-3.70	5.70	1.58	1.70	1.89
Spring	*INSIDE*					
	Temperature [°C]	20.70	30.80	24.31	24.10	2.51
	Humidity [%]	78.00	96.00	87.46	86.00	4.24
	OUTSIDE					
	Temperature [°C]	15.30	31.30	21.83	21.75	4.08
	Humidity [%]	36.00	99.00	70.78	70.00	17.41
	Absolute pressure [mmHg]	743.00	747.70	744.75	744.50	1.02
	Wind speed [m/s]	0.00	4.80	1.69	1.70	0.96
	Dew point [°C]	11.80	19.40	15.76	15.70	1.23

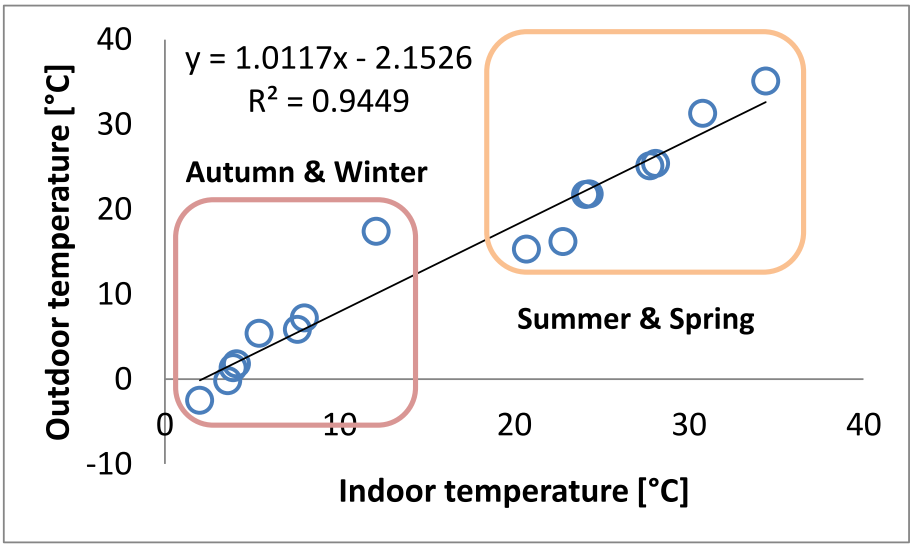

a)

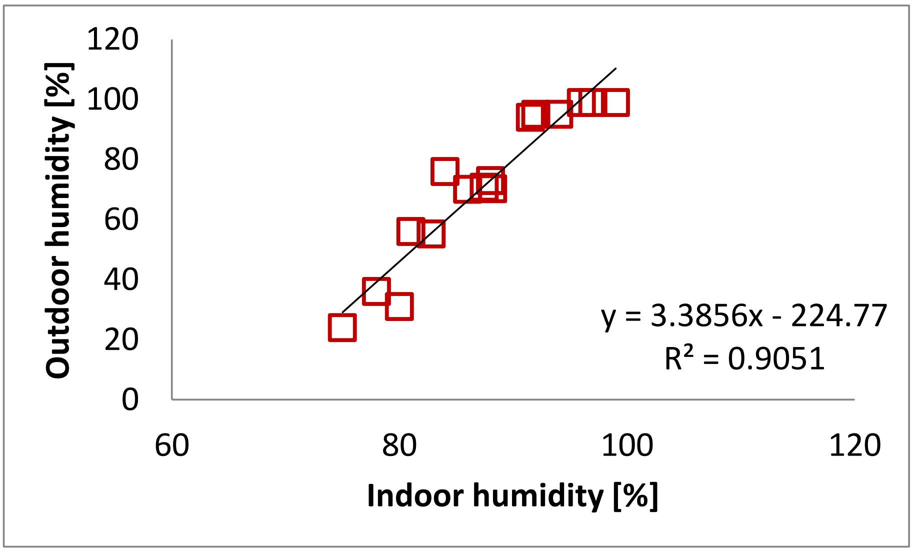

b)

Figure 1. a) Linear correlation between inside and outside temperature; b) Polynomial correlation between inside and outside humidity.

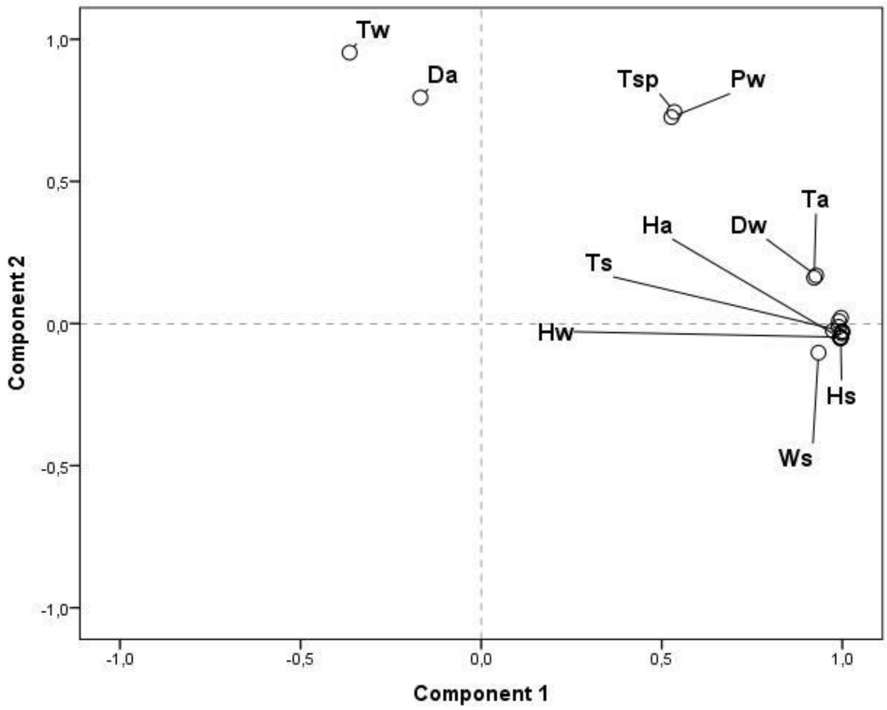

Figure 2. Principal component analysis by Component plot in rotated space of microclimate parameters: Ts – temperature in summer; Ta – temperature in autumn; Hs – humidity in summer; Ha – humidity in autumn; Ps – absolute pressure in summer; Pa – absolute pressure in autumn; Ws – wind speed in summer; Wa – wind speed in autumn; Ds – dew point in summer; Da – dew point in autumn.

Table 2. Correlation matrix of microclimate parameters measured outside in both summer and autumn seasons: Ts – temperature in summer; Ta – temperature in autumn; Hs – humidity in summer; Ha – humidity in autumn; Ps – absolute pressure in summer; Pa – absolute pressure in autumn; Ws – wind speed in summer; Wa – wind speed in autumn; Ds – dew point in summer; Da – dew point in autumn (the bold text highlights the microclimate parameters with strong correlation >0.9; the italic text highlights the microclimate parameters with good correlation 0.7-0.9).

	Ts	Ta	Tw	Tsp	Hs	Ha	Hw	Hsp	Ps	Pa	Pw	Psp	Ws	Wa	Ww	Wsp	Ds	Da	Dw	Dsp
Ts	1																			
Ta	**0.907**	1																		
Tw	-0.326	-0.147	1																	
Tsp	0.581	0.555	0.547	1																
Hs	**0.998**	*0.881*	-0.342	0.579	1															
Ha	**0.998**	*0.877*	-0.343	0.579	**1**	1														
Hw	**0.998**	*0.880*	-0.341	0.580	**1**	**1**	1													
Hsp	**0.998**	*0.880*	-0.342	0.579	**1**	**1**	**1**	1												
Ps	**0.998**	*0.876*	-0.344	0.579	**1**	**1**	**1**	**1**	1											
Pa	**0.998**	*0.877*	-0.344	0.579	**1**	**1**	**1**	**1**	**1**	1										
Pw	0.575	0.526	0.535	**0.998**	0.576	0.577	0.578	0.577	0.577	0.577	1									
Psp	**0.999**	**0.912**	-0.280	0.618	**0.997**	**0.996**	**0.996**	**0.996**	**0.996**	**0.996**	0.611	1								
Ws	**0.907**	**0.965**	-0.398	0.345	*0.885*	*0.881*	*0.884*	*0.884*	*0.881*	*0.881*	0.319	*0.899*	1							
Wa	**0.958**	**0.977**	-0.332	0.471	**0.941**	**0.938**	**0.940**	**0.940**	**0.938**	**0.938**	0.450	**0.954**	**0.988**	1						
Ww	**0.978**	**0.968**	-0.319	0.517	**0.965**	**0.963**	**0.964**	**0.964**	**0.963**	**0.963**	0.500	**0.976**	**0.972**	**0.996**	1					
Wsp	**0.981**	**0.968**	-0.301	0.538	**0.968**	**0.966**	**0.967**	**0.967**	**0.966**	**0.966**	0.522	**0.980**	**0.966**	**0.995**	1	1				
Ds	**1**	**0.907**	-0.330	0.576	**0.998**	**0.998**	**0.998**	**0.998**	**0.998**	**0.998**	0.570	**0.999**	**0.909**	**0.959**	**0.979**	**0.981**	1			
Da	-0.174	0.212	*0.760*	0.324	-0.222	-0.229	-0.223	-0.224	-0.230	-0.230	0.279	-0.141	0.024	0.003	-0.036	-0.030	-0.175	1		
Dw	**0.914**	1	-0.141	0.571	*0.889*	*0.885*	*0.888*	*0.887*	*0.884*	*0.885*	0.543	**0.919**	**0.962**	**0.978**	**0.971**	**0.971**	**0.914**	0.204	1	
Dsp	**1**	*0.896*	-0.331	0.581	**0.999**	**0.999**	**0.999**	**0.999**	**0.999**	**0.999**	0.577	**0.998**	*0.898*	**0.951**	**0.973**	**0.976**	1	-0.194	**0.904**	1

The ICP-MS analysis was highlighted a rich particles content in iron (6.06–7.25 ng·m^{-3} inside and 75.90–107.80 ng·m^{-3} outside) and manganese (3.10–5.17 ng·m^{-3} inside and 12.80–23.80 ng·m^{-3} outside) (Table 3) and this demonstrated an accelerated oxidation process [30] on the surface of ruins structure.

Table 3A. Descriptive statistics of metals content (expressed as ng/m^3), measured daily by ICP-MS, one week per season (inside of the Tropaeum Traiani Monument).

	Metals	Min.	Max.	Mean	Median	S.D.
Summer	^{27}Al	2.24	3.16	2.47	2.35	0.41
	^{52}Cr	0.21	0.38	0.30	0.30	0.07
	^{55}Mn	4.26	5.17	4.84	4.93	0.39
	^{57}Fe	6.20	7.13	6.69	6.86	0.39
	^{60}Ni	1.24	1.63	1.41	1.41	0.16
	^{63}Cu	1.28	1.54	1.43	1.49	0.11
	^{66}Zn	5.84	7.31	6.64	6.73	0.60
	^{111}Cd	0.10	0.14	0.13	0.13	0.02
	^{208}Pb	0.59	0.70	0.63	0.62	0.05
Autumn	^{27}Al	1.35	1.81	1.55	1.44	0.20
	^{52}Cr	0.17	0.36	0.23	0.20	0.08
	^{55}Mn	3.10	4.34	3.89	4.07	0.53
	^{57}Fe	6.06	7.25	6.71	6.56	0.49
	^{60}Ni	0.76	0.95	0.83	0.80	0.08
	^{63}Cu	0.70	0.92	0.79	0.73	0.10
	^{66}Zn	3.75	7.01	5.93	6.30	1.41
	^{111}Cd	0.05	0.08	0.06	0.06	0.01
	^{208}Pb	0.35	0.41	0.38	0.39	0.03
Winter	^{27}Al	0.69	0.92	0.79	0.73	0.10
	^{52}Cr	0.13	0.27	0.18	0.16	0.06
	^{55}Mn	3.06	4.28	3.84	4.02	0.52
	^{57}Fe	1.87	2.24	2.07	2.03	0.15
	^{60}Ni	0.78	0.96	0.84	0.81	0.08
	^{63}Cu	0.95	1.24	1.07	0.99	0.13
	^{66}Zn	0.65	1.21	1.03	1.09	0.24
	^{111}Cd	0.12	0.19	0.15	0.15	0.03
	^{208}Pb	1.02	1.21	1.12	1.14	0.08
Spring	^{27}Al	0.79	1.09	0.90	0.84	0.13
	^{52}Cr	0.23	0.45	0.32	0.31	0.09
	^{55}Mn	3.70	4.88	4.45	4.61	0.50
	^{57}Fe	2.03	2.39	2.22	2.21	0.15
	^{60}Ni	1.26	1.60	1.40	1.37	0.14
	^{63}Cu	1.35	1.70	1.51	1.48	0.14
	^{66}Zn	1.09	1.67	1.46	1.52	0.25
	^{111}Cd	0.17	0.24	0.20	0.20	0.03
	^{208}Pb	1.18	1.39	1.28	1.28	0.09

The higher content of metals (Table 3) was detected in suspended particulate matter collected in August 2018, in comparison of those sampled in November 2018. Regarding the place, inside and outside of monument, the content of investigated metals (*i.e.*, Pb, Cd, Cr, Ni, Cu, Mn, Al, Zn and Fe) was higher outside and this finding may result from the fact that most of metals are accumulated in the finest fraction of $PM_{2.5\text{-}10}$. Particularly, in the summer of 2018, the high concentrations were measured in case of manganese, iron, and zinc (Table 3). In autumn 2018, these metals concentration was less than summer, due to the raining and cold period of the end of November. As reported by different studies [15,18], Al, Fe, Mn, Al, Zn, Ba, Sr, Ca, Mg and Ti were found mainly in coarse particles, while Cr, Ni, Co, Cu, Zn, Cd, Pb, As and Se occurred specially in fine particulate matter ($PM_{2.5–10}$). Previous research [19] highlights that element mostly concentrated in accumulation mode are S, As (with chemical speciation), Se, Ag, Cd, Tl and Pb and the elements having multimode distribution are Be, Na, K, Cr, Mn, Co, Ni, Cu, Zn, Ga, Mo, Sn and Sb.

The measured values of element amount expressed as maximum, minimum, median, mean in analyzed particulate matters were ~4–13 times higher for all metals outside comparative with the values obtained for samples collected inside of historical monument.

On the other hand, the ironrich particles are good catalyst with sulfur-containing substances to form into sulfuric acid or other sulfate salts [34-38] to enhance the corrosion process of the monuments structure. The presence of sulfate, carbonate, ammonium, and nitrate groups, as well as organic functional groups such as aliphatic carbons, carbonyls, and organic nitrates in samples collected in summer and autumn, respectively, was identified by nondestructive ATR-FTIR technique, according with data presented in Table 4.

Table 3B. Descriptive statistics of metals content (expressed as ng/m^3), measured daily by ICP-MS, one week per season (outside of the Tropaeum Traiani Monument).

	Metals	Min.	Max.	Mean	Median	S.D.
Summer	^{27}Al	3.90	5.50	4.30	4.10	0.72
	^{52}Cr	1.61	2.90	2.27	2.30	0.53
	^{55}Mn	19.60	23.80	22.28	22.70	1.78
	^{57}Fe	93.80	107.80	101.14	103.80	5.90
	^{60}Ni	7.50	9.80	8.48	8.50	0.94
	^{63}Cu	7.60	9.10	8.44	8.80	0.65
	^{66}Zn	71.90	89.90	81.66	82.80	7.40
	^{111}Cd	0.90	1.20	1.10	1.10	0.13
	^{208}Pb	5.80	6.80	6.16	6.10	0.42
Autumn	^{27}Al	2.90	3.90	3.34	3.10	0.43
	^{52}Cr	0.68	1.43	0.93	0.82	0.33
	^{55}Mn	12.80	17.90	16.04	16.80	2.19
	^{57}Fe	75.90	90.80	84.02	82.10	6.14
	^{60}Ni	4.60	5.70	4.98	4.80	0.48
	^{63}Cu	4.90	6.40	5.52	5.10	0.67
	^{66}Zn	33.90	63.30	53.60	56.90	12.67
	^{111}Cd	0.60	0.90	0.74	0.70	0.12
	^{208}Pb	4.30	5.10	4.72	4.80	0.33
Winter	^{27}Al	0.91	1.22	1.04	0.97	0.13
	^{52}Cr	0.17	0.36	0.23	0.21	0.08
	^{55}Mn	4.04	5.65	5.06	5.30	0.69
	^{57}Fe	24.47	28.96	27.74	26.68	2.20
	^{60}Ni	1.02	1.27	1.11	1.07	0.11
	^{63}Cu	1.26	1.64	1.41	1.31	0.17
	^{66}Zn	20.86	21.60	21.36	21.44	2.32
	^{111}Cd	0.16	0.25	0.20	0.19	0.03
	^{208}Pb	1.35	1.60	1.48	1.51	0.10
Spring	^{27}Al	1.10	1.51	1.24	1.17	0.18
	^{52}Cr	0.32	0.62	0.45	0.43	0.12
	^{55}Mn	5.14	6.77	6.17	6.39	0.70
	^{57}Fe	27.81	32.32	31.08	30.07	2.21
	^{60}Ni	1.75	2.23	1.93	1.90	0.20
	^{63}Cu	1.88	2.35	2.10	2.05	0.20
	^{66}Zn	21.52	22.32	22.03	22.11	2.34
	^{111}Cd	0.23	0.33	0.28	0.27	0.04
	^{208}Pb	1.63	1.93	1.77	1.78	0.12

Based on FTIR spectra the molecular characteristics in multicomponent PM was studied, as well as the changes to composition under different climatic conditions (*e.g.*, humidification, oxidation) providing insight into atmospherically relevant aerosol processes. FTIR spectra were acquired rapidly and nondestructively from PTFE filters, which are commonly used for gravimetric mass analysis in regulatory monitoring. After correction for the background spectrum was made, all analyzed spectra showed weak and medium vibrational frequencies (Table 4) around 615w and 1130m cm^{-1} for SO_4^{2-} ions. The weak and medium peaks around 820w cm^{-1} and 1360m cm^{-1} were assigned to NO_3^- ions, and those from 1460 cm^{-1} corresponding to NH_4^+ cations. The strong signals around 712s cm^{-1} were attributed to geogenic CO_3^{2-} ions derived from local carbonate rocks. Vibrational assignments around 870w cm^{-1}, 1395s cm^{-1} 1465s/m cm^{-1} and 1792w cm^{-1}, correspond to CO_3^{2-} ions, as well. SiO_4^{4-} ions, identified by the weak and medium or strong peaks around 439w cm^{-1}, 465w cm^{-1} and 1040s/m cm^{-1}, respectively were detected mainly in samples collected in the summer of 2018 (Table 4).

Table 4. Tentative assignments of significant peak from FTIR spectra; S1-S7 represents PM samples collected on summer season; A1-A7 represents PM samples collected on autumn season; all data sets were performed inside of Tropaeum Traiani Monument.

Summer							Autumn							
S1	**S2**	**S3**	**S4**	**S5**	**S6**	**S7**	**A1**	**A2**	**A3**	**A4**	**A5**	**A6**	**A7**	**Assignment**
Wavenumber [cm^{-1}] & relative intensity*														
3362 w	3363 w	3362 w	3365 w	3361 w	3369 w	3367 w	3365 m	3357 m	3361 m	3363 m	3356 m	3361 m	3363 m	stretching O-H
1792 w	1793 w	1796 w	1795 w	-	1796 w	1794 w	1791 w	1795 w	-	1795 w	1798 w	1790 w	1792 w	C-O (CO_3^{2-})
-	1632 m	-	-	1639 m	-	-	1637 m	1639 m	1647 s	1635 s	1629m	1635 m	1639 m	C-NH_2 (amine)
1465 m	1463 s	1465 m	1465 m	1462 m	1464 m	1461 m	1463 s	1461 s	1462 s	1460 m	1462 m	1465 m	1463 m	N-H (NH_4^+) and C-O (CO_3^{2-})
1393 s	-	1391 s	1392 s	1393 s	1408 s	-	-	-	-	-	1395 s	1392 s	1394 s	C-O (CO_3^{2-})
1363 m	1368 m	1368 m	1364 m	1361 m	1360 m	1363 m	1367 m	1362 w	1365 w	1365 w	1364 m	1361 m	1367 m	N-O (NO_3^-)
1131m	1130m	1138 m	1127 m	1130m	1123m	1132m	1127 m	1128 w	1130m	1122w	1123m	1127 w	1129 m	S-O (SO_4^{2-})
1040 s	1043 s	1035 s	1040 s	1036 m	1042 m	1035 m	1038 m	1039 m	1041 m	1039 m	1037 m	1038 m	1040 m	Si-O (SiO_4^{4-})
870s	874s	875s	876 m	873s	873s	873s	873s	873s	873s	872s	872s	872s	871s	C-O (CO_3^{2-})
820 w	817 w	825 w	821 w	823 w	823 w	821 w	818 w	821 w	819 w	822 w	-	820 w	-	N-O (NO_3^-)
796 m	794 m	797 m	794 m	795 m	800 m	796 m	796 w	797 w	-	-	-	-	-	Si-O (quartz)
781s	781s	778s	777s	780s	778 m	781 m	778 w	780 w	-	-	-	-	-	Si-O (quartz)
711s	712s	713s	712s	712 m	712s	712s	712s	712s	712 m	712s	712s	712s	712s	Ca-O ($CaCO_3$)
618 w	614 w	614 w	616 w	615 w	618 w	612 w	615 w	614 w	617 w	615 w	612 w	616 w	610 w	S-O (SO_4^{2-})
465 m	-	461 w	469 w	465 w	464 w	-	460s	-	-		467 w	-	-	Si-O (SiO_4^{4-})
431 w	444s	439 w	439s	445s	443 w	-	447 w	-	445 w	-	431 w	-	445 w	Si-O (SiO_4^{4-})
-	-	427 w	-	-	420 w	426 w	-	-	429 w	-	-	-	429 w	Ti-O (rutile)
406 m	412 m	416 m	402 m	417 m	400 m	414 w	-	398s	390s	399 m	-	398 m	394s	Si-O (quartz)

** s - strong; m - medium; w – weak.*

The medium or strong peaks, around 400m cm^{-1} and 777s/m – 797m cm^{-1}, were attributed to Si-O from quartz, which is present in all samples collected in August of 2018. FTIR also identified several organic functional groups, although specific organic molecules could not be identified. The broad bands in the region 3357–3367 cm^{-1} are assigned to OH-stretching mainly from water.

4. CONCLUSIONS

As a premiere for Romanian cultural heritage, it been made a complex investigation over the monument degradation causes and was asset a correlation between monitored climatic factors and results obtained by different analytical techniques (ICP-MS and ATR-FTIR). This research is a first step of an ambitious project, based on a complex acquisition of microclimatic data during a long-term monitoring (*i.e*,. on three complete seasons). The investigations and obtained results are representative for old historical monuments of Romania, rehabilitated without preliminary scientific studies on building materials and climatic changes.

With respect to the analysis carried out on the risks for the conservation and rehabilitation of historical monument the mainly microclimatic parameter, a real danger for the conservation of the material structure, is humidity, due to its significant and repeated variations during of seasons of the years 2018 and 2019. Throughout monitoring periods, values of temperature and humidity exceeded the values for the same periods of last year. In this respect, climatic effects due to seasonal changes are the reason for temperature variation and humidity high values which also increasing the chances of fungus and perennial plant occurrence. The degradation phenomena including soiling, are currently taking place not only to the surface of original material from inside of the monument, but on metallic materials as well (structure of reconstruction), which are affected by corrosion phenomena. The monitoring data collected is the main source of information for carrying out a risk analysis, and for the future achievement of new materials for rehabilitation and conservation of historical monuments supported through further studies.

Acknowledgments: *This work was supported by a project of the Romanian National Authority for Scientific Research, UEFISCDI, project 51PCCDI/2018 "New diagnosis and treatment technologies for the preservation and revitalization of archaeological components of the national cultural heritage".*

REFERENCES

[1] Florescu, R., *Adamclisi*, Meridiane, Bucharest, 1983.
[2] Jones, M.W., *Principles of Roman Architecture*, Yale University Press, New Haven, 2003.
[3] Hannestad, N., *Roman Art and Imperial Policy*, Aarhus University Press, Aarhus, 1988.
[4] Hannestad, N., In *Ateliers and Artisans in Roman Art and Archaeology*, Vol. 92, Kristensen, T.M. and Poulsen, B. (Eds.), *Journal of Roman Archaeology*, Cambridge, p. 77, 2012.
[5] Covacef, Z., *Arta sculpturală în Dobrogea Romană, secolele I-III*, Nereamia Napocae, Cluj-Napoca, 2002
[6] Bonazza, A., Messina, P., Sabbioni, C., Grossi, C.M., Brimblecombe, P., *Sci Total Environ*., **407**(6), 2039, 2009.
[7] Grau-Bove, J., Strlic, M., *Herit. Sci*., **1**, 8, 2013.
[8] Nazaroff, W.W., Ligocki, M.P., Ma, T., Cass, G.R., *Aerosol Sci Technol*., **13**(3), 332, 1990.
[9] Camuffo, D., *Sci. Total Environ*., **167**, 1, 1995.
[10] Hu, T., Lee, S., Cao, J., Chow, J.C., Watson, J.G., Ho, K., Ho, W., Rong, B., An, Z., *Sci Total Environ*., **407**(20), 5319, 2009.

[11] Mastromei, G., Microbes and Art: The role of microbial communities in the degradation and protection of cultural heritage, Plenum, New York, 2000.
[12] Gysels, K., Delalieux, F., Deutsch, F., Camuffo, D., Bernardi, A., Sturaro, G., Busse, H.J., Wieser, M., Van Grieken, R., *J. Cult. Herit*., **5**(2), 221, 2004.
[13] Samek, L., Maeyer-Worobiec, A.D., Spolnik, Z., Bencs, L., Kontozova, V., Bratasz, L., Kozlowski, R., Van Grieken, R., *J. Cult. Herit*., **8**(4), 361, 2007.
[14] Casati, M., Rovelli, G., D'Angelo, L., Perrone, M.G., Sangiorgi, G., Bolzacchini, E., Ferrero, L., *Aerosol Air. Qual. Res*., **15**, 399, 2015.
[15] Radulescu, C., Stihi, C., Iordache, S., Dunea, D., Dulama, I.D., *Rev Chim (Bucharest)*, **68**(4), 805, 2017.
[16] Dunea, D., Iordache, S., Radulescu, C., Pohoata, A., Dulama, I.D., *Rom. J. Phys*., **61**(7-8), 1354, 2016.
[17] Iordache, S., Dunea, D., Radulescu, C., Dulama, I.D., Ianache, R., Predescu, M., *Rev Chim (Bucharest)*, **68**(4), 879, 2017.
[18] Radulescu, C., Iordache, S., Dunea, D., Stihi, C., Dulama, I.D., *Rom. J. Phys*., **60**(7-8), 1171, 2015.
[19] Radulescu, C., Stihi, C., Dulama, I.D., Elemental analysis methods for particulate matter. Chemical speciation. Analytical method validation. In *Methods for the Assessment of Air Pollution with Particulate Matter to Children's Health*, Iordache, S. and Dunea, D. (Eds.), MatrixRom, Bucharest, p.119, 2014.
[20] Sahan, E., ten Brink, H.M., Weijers, E.P., Carbon in atmospheric particulate matter – Technical report (DOI: 10.13140/RG.2.1.2020.1444). ECN Energy Research Centre of the Netherlands, Petten, 2008.
[21] Viana, M., Diez, S., Reche, C., *Atmos. Environ*., **45**(35), 6359, 2011.
[22] Lu, H.Y., Mwangi, J.K., Wang, L.C., Wu, Y.L., Tseng, C.Y., Chang, L.H., *Aerosol Air Qual. Res*., **16**, 2488, 2016.
[23] Spolnik, Z., Worobiec, A., Samek, L., Bencs, L., Belikov, K., Van Grieken, R., J. *Cult. Herit*., **8**, 7, 2007.
[24] Pipal, A.S., Jan, R., Satsangi, P.G., Tiwari, S., Taneja, A., *Aerosol Air Qual. Res*., **14**, 1685, 2014.
[25] Mouratidou, T., Samara, C., *Atmos. Environ*., **38**(27), 4593, 2004.
[26] Koponen, I.K., Asmi, .A, Keronen, P., Puhto, K., Kulmala, M., *Atmos. Environ*., **35**(8), 1465, 2001.
[27] Kendall, M., Hamilton, R.S., Watt, J., Williams, I.D., *Atmos. Environ*., **35**(14), 2483, 2001.
[28] Liu, X., Li, C., Tu, H., Wu, Y., Ying, C., Huang, Q., Wu, S., Xie, Q., Yuan, Z., Lu, Y., *Aerosol Air Qual. Res*., **16**, 3222, 2016.
[29] Bernardi, A., Camuffo, D., Microclimate in the Chiericati Palace Municipal Museum, Vicenza. Mus. Manage Curatorship., **14**, 5, 1995.
[30] Radulescu, C., Stihi, C., Ion, R.-M., et al., *Atmosphere*, **10**(10), 595, 1, 2019.
[31] Ion, R.M., Iancu L., Grigorescu R.M. et al., *J. Sci. Arts,*, **2**(43), 471, 2018
[32] Olteanu R.L., Radulescu C., Stihi C., et al., *J. Sci. Arts*, **4**(53), 977, 2020
[33] Bintintan A., Gligor M., Radulescu C., et al., *Anal. Lett.*, **52**(15), 2348, 2019
[34] Maria, S.F., Russel, L.M., Turpin, B.L., Porcja, R.J., *Atmos. Environ*., **36**, 5185, 2002.
[35] Khoder, M.I., *Chemosphere*, **49**, 675, 2002.
[36] Spolnik, Z., Worobiec, A., Injuk, J., et al., *Microchim. Acta*, **145**, 223, 2004.
[37] Bintintan, A., Gligor, M., Dulama, I.D., Radulescu, C., Stihi, C., Ion, R.M., Teodorescu, S., Stirbescu, R.M., Bucurica, I.A., Pehoiu, G., *Rom. J. Phys.*, **64**(5-6), 903, 2019.
[38] Tomus (Szabo), D.E., Gligor, M., Dulama, I.D. et al., *J. Sci. Arts*, **1**(54), 285, 2021